X-ray Standing Wave Studies of Underpotentially Deposited Metal Monolayers

G. M. Bommarito, D. Acevedo, J. F. Rodríguez and H. D. Abruña*
Department of Chemistry
Baker Laboratory, Cornell University
Ithaca, New York 14853-1301
and
T. Gog and G. Materlik
HASYLAB at DESY
Notkestraße 85
2000 Hamburg 52
Germany

ABSTRACT

The x-ray standing wave technique has been employed in the study of the structure of underpotentially deposited (UPD) copper on an iodine covered platinum surface and of copper on a Au(100) single crystal electrode. For Cu UPD on Pt, surface coverage isotherms derived from both electrochemical and x-ray measurements are compared. The growth mode of the copper ad-layer appears to be strongly influenced by the electrode's surface morphology. For Cu UPD on Au(100) the coherence of the adlayer is strongly dependent on the mode of deposition.

INTRODUCTION

The process of underpotential deposition (UPD) of metals has been extensively studied during the past two decades due to its theoretical and practical importance.[1] In this process, submonolayer to monolayer(s) amounts of a metal can be electrodeposited on a foreign metal substrate in a quantifiable and reproducible fashion prior to bulk deposition. Numerous electrochemical and spectroscopic techniques have been utilized to probe the mechanism(s) of formation, and the structural properties of UPD layers. Conventional electrochemical methods have been used to obtain thermodynamic and kinetic information about the UPD process [1-3]. Although electrochemical methods are invaluable in controlling and measuring thermodynamic parameters, structural inferences are always indirect and often model dependent.

Surface sensitive ultra high vacuum techniques have been employed in the study of such systems and much information has been obtained from them [4]. However, the fact that these studies are inherently ex-situ raises some fundamental questions as to their applicability.

In recent years, the use of atomic resolution microscopic techniques has provided the means to obtain in-situ direct atomic structural information from UPD

systems. Scanning tunneling and atomic force microscopy have been recently employed in the study of UPD processes [5]. These studies have shown that, in general, the UPD process occurs in a well-defined manner and that the structures observed from these experiments are similar to those observed in vacuum. As was the case in the ex-situ experiments, these techniques provide information only for the deposited layer.

Recently, in situ x-ray spectroscopic and diffraction techniques have provided unique atomic resolution structural information about UPD systems [6]. Extended x-ray absorption fine structure (EXAFS) and x-ray absorption near edge structure (XANES) have been widely used to study various UPD systems [7], providing information about the local structure atomic environment and the oxidation state of the adsorbed species. Furthermore, surface x-ray scattering measurements have been used to study the in-plane structure of various UPD systems [8]. X-ray standing waves (XSW) [9-12] have also been utilized to probe the structure of UPD layers and were the first x-ray experiments to demonstrate the applicability of these techniques in-situ and ex-situ [9]. In addition, this technique allows one to obtain information pertaining to the distribution of species, including the diffuse layer, in a direction normal to the substrate's surface.

In this paper, we present the results of a series of x-ray standing wave experiments aimed at probing the potential dependent structural nature of the underpotential deposition of copper on an iodine covered platinum surface and of copper underpotentially deposited on a Au(100) single crystal electrode.

THEORETICAL BACKGROUND

X-ray standing waves are generated when coherently related incident and reflected plane waves interfere.[13] The standing wave electric field intensity is given by:

$$I(\theta,z) = |\bar{\varepsilon}_o + \bar{\varepsilon}_R|^2 = |E_O|^2 \, [1+R+2\sqrt{R}\cos(\nu-2\pi Q_z)], \qquad (1)$$

where $\bar{\varepsilon}_o$ and $\bar{\varepsilon}_R$ are the incident and reflected plane waves if their respective wavevectors k_O and k_R lie in the x-z plane with the z axis normal to the substrate's surface. $Q = k_O - k_R$ is the momentum transfer with a magnitude given by:

$$|Q| = Q = 2 \sin\theta/\lambda = 1/D, \qquad (2)$$

At the Bragg angle (θ_B), the scattering vector is a reciprocal lattice vector $\vec{H}$ with $|\vec{H}|=1/d_H$ where d_H is the substrate's characteristic d-spacing of reflection $\vec{H}$. The angular dependence of equation (1) is contained within the variables $R(\theta)$ and $\nu(\theta)$ which correspond, respectively, to the intensity and the phase of the reflected wave relative to the incident one. During specular reflection (total external reflection) [14] and Bragg diffraction, a strong and well-defined standing wave field is generated. In addition, as the angle of incidence θ is scanned across these reflection regimes, there is a change of π in the relative phase $\nu(\theta)$, causing the nodal and antinodal planes of the standing wave field to move inward in a direction normal to the substrate's surface (we confine our discussion here to the case where the diffraction planes of the substrate are parallel to the surface). Since the photoelectric effect for core electrons is directly proportional, in the dipole approximation, to the electric field intensity at the center of an atom, the emission yield (i.e. the fluorescence yield) from the atoms in an overlayer or in a distribution of species above the substrate's surface will be uniquely modulated as a

function of θ. To calculate this yield, the standing wave electric field intensity I(z,θ) must be integrated over the entire distribution N(z):

$$Y(z,\theta) = \int I(z,\theta)\, f(z)\, dz \qquad (3)$$

Conventionally, XSWs are generated by dynamical Bragg diffraction from perfect single crystals [13,15]. In this work, we are interested in studying structural changes not only for an atomic overlayer but also for extended distributions of species (on the order of tens to hundreds of Å). Thus, depending on the length scale of interest, we have employed two different substrates. In the study of Cu UPD on an iodine covered Pt surface we employed Pt/C layered synthetic microstructures (LSM) with characteristic d-spacings of the order of 40Å as both the electrode and the diffracting structure. LSMs are artificial, depth-periodic structures [16], prepared by depositing alternating layers of high and low electron density elements, thus creating a superlattice structure with diffraction planes centered in the high electron density layers. The XSW technique using LSMs has been applied in several studies [10-12], and we refer the reader to these references for further details.

In the case of copper UPD on gold, we employed a single crystal Au(100) grown from the melt and prepared so as to have a very low density of dislocations. [17].

EXPERIMENTAL

Experiments of Cu UPD on an iodine treated Pt surface were carried out at the Cornell High Energy Synchrotron Source (CHESS) using the B2 beam line employing a double-crystal Si(111) monochromator.

The electrochemical cell, housed inside an aluminum holder, consisted of a cylindrical Teflon body with feedthroughs for electrolytes and electrode connections. The cell was thoroughly cleaned prior to use. The filling and rinsing of the cell with electrolyte was accomplished with pressurized glass vessels through the fluid feedthroughs. A thin layer of solution (approx. 1-3 mm thick) was trapped between the electrode, and a 6.35 mm thick polypropylene film which was held in place by a Teflon ring. All the electrochemical measurements were conducted with the polypropylene film distended by the addition of excess bulk electrolyte into the cell. The thin layer was then restored by removing excess electrolyte. Potential control of the electrode was retained through filling and rinsing stages. All applied potentials are reported with respect to a Ag/AgCl reference electrode.

Platinum/carbon LSMs of dimensions 15 mm by 20 mm were obtained from Ovonic Synthetic Materials Co. (Troy, MI). The LSMs used had d-spacings of 39.7 Å or 41.4 Å, and consisted of 200 layer pairs of platinum and carbon with platinum as the outermost layer, deposited on a 0.015 in. thick Si(111) substrate.

Solutions were prepared with ultrapure reagents (Aldrich, Baker, Alfa) and pyrolytically distilled water (PDW). Prior to use, solutions were degassed for over 30 min. with high purity nitrogen which was passed through hydrocarbon and oxygen traps. The electrolyte was 0.10 M sulfuric acid (Baker Ultrex) containing 1×10^{-4} M copper sulfate (Aldrich Gold Label) and was prepared using pyrolytically distilled water.

The Pt/C LSM was cleaned by a series of oxidation-reduction cycles (at 20mV/sec) in pure supporting electrolyte (0.1M sulfuric acid) followed by formation of the iodine ad-layer which was formed by contacting the electrode with a 1mM solution of NaI in 0.1M sulfuric acid for 15 min. Afterwards, the electrode was rinsed with supporting electrolyte. Prior to copper deposition, electrolyte solution was added to the

cell so that the polypropylene film distented somewhat, thus allowing the UPD layer to be deposited from bulk electrolyte. The monolayer was deposited from bulk electrolyte because of the low copper concentration. Deposition was carried out at constant potential for 15 min. after which the current had decayed to background levels. Deposition potentials of +0.45, +0.25, +0.20, +0.15 and +0.10 vs Ag/AgCl were employed and these corresponded to copper coverages of 0, 1/4, 1/2, 3/4 and a full monolayer, respectively. After deposition, part of the electrolyte solution was withdrawn, leaving only a thin layer of electrolyte, whose thickness we estimate from reflectivity measurements to be of the order of 5 microns, between the electrode and the polypropylene film. The amount of copper ions contained within the thin layer represents about 2-5% of the amount electrodeposited on the surface. As a result, no interference from copper in solution was anticipated.

For each XSW scan, an energy-dispersed fluorescence spectrum at a given angular position was recorded into 256 channels of a LeCroy histogramming memory module. A typical scan consisted of 64 points over angular ranges of 10 mrad and 3.75 mrad for the specular reflection and Bragg diffraction regions respectively, and took approximately 20 min. to complete. Approximately 2 min/point of data were collected for each potential studied.

In the study of Cu UPD on Au(100), the electrode was placed in a thoroughly degassed solution of 0.1M H_2SO_4 and the potential was scanned at 20 mV/sec until the characteristic voltammetric profile was obtained[18]. The electrode was then placed in a thoroughly degassed solution of 0.1M H_2SO_4 containing copper at either 1mM or 50μM concentration and the potential was scanned over the UPD region [19]. The potential was held at the desired value for a prescribed amount of time until the current had decayed to background levels. The electrode was removed from the solution under potential control and rinsed thoroughly with water. It was subsequently mounted on a Huber Euler cradle where the XSW experiments were carried out.

The XSW studies of Cu UPD on Au(100) were carried out at the Hamburger Synchrotronstrahlungslabor (HASYLAB) on Beam line Römo I. A Ge(220) and an asymmetrically cut (17°) Si(220) double crystal monochromator were used to select an incident energy of 10.54keV. This value was sufficient to excite CuK_α fluorescence, but below that of all the gold L edges, thus minimizing the background signal. Data acquisition was done with the program SPECTRA in conjunction with LeCroy histogramming memory modules.

It should be emphasized that while the studies of Cu UPD on an iodine treated platinum surface were carried out in-situ, the work on Cu UPD on Au(100) was ex-situ.

1. X-Ray Standing Wave Study of Cu UPD on an Iodine Treated Pt Surface:

A. Surface coverage Isotherms:

In these experiments, a platinum/carbon LSM is used as the diffracting substrate and working electrode. In sulfuric acid media, the voltammetry due to the platinum surface of the LSM exhibited only one pronounced (the so-called weakly bound) hydrogen adsorption peak. Such behavior has been previously shown to be characteristic of a clean well-ordered Pt(111) electrode that has been cycled into the oxide region a few times to yield a Pt(111) surface with nearly randomly distributed monatomic steps [20]. In fact, the voltammetry for copper UPD on the iodine treated LSM (Figure 1) was virtually identical to that of an iodine coated Pt(111) electrode that was treated as mentioned above. As mentioned previously, x-ray measurements were carried out at applied potentials of +0.45, +0.25, +0.20, +0.15 and +0.10 corresponding to copper surface coverages of approximately 0, 1/4, 1/2, 3/4 and 1 monolayer, respectively.

Copper surface coverages were determined from both electrochemical and x-ray fluorescence measurements. Electrochemically, the coverage was determined from integration of the area under the voltammetric wave. Surface coverage isotherms from two different sets of experiments were obtained. In the first, the deposited copper was stripped in the presence of bulk copper whereas in the second case the electrode was rinsed three times with supporting electrolyte containing no copper. Comparing these isotherms, we observe a loss of deposited copper, after rinsing, that is coverage dependent. At full monolayer coverage the loss was only 16% whereas at sub-monolayer coverages of 3/4, 1/2 and 1/4 the losses were 47, 55 and 62%, respectively.

In the x-ray measurements, the coverage isotherms were determined from the off-Bragg fluorescence yield data of the XSW measurements. (Note: Such off-Bragg (i.e. away from the Bragg angle) yield experiments essentially measure all the copper species contained within the thin layer of liquid trapped between the electrode and a polypropylene film which serves as a window.) We carried out rinsing and no rinsing experiments equivalent to the ones described above. Again, we observe a drastic loss of surface coverage after rinsing the electrode. However, the fractional losses are considerably larger than those measured electrochemically. In an attempt to compare these experiments, the x-ray derived isotherms have been plotted on an absolute scale versus the electrochemical ones normalizing the two data sets at only one point: +0.10V, for the rinsing experiments (Figure 2). We note that the coverage isotherms for the rinsing case for both the x-ray and electrochemical experiments are in excellent agreement, but when we compare the results of experiments where the electrode had not been rinsed, the x-ray measurements indicate the presence of a considerable amount of electrochemically inactive copper, above and beyond the bulk copper present in solution. In addition, XSW measurements corresponding to this coverage place this excess copper at the solid/solution interface. Furthermore, even at applied potentials of +0.45 V, where no electrodeposition has yet occurred, we observe an amount of copper equivalent to approximately 20% of a monolayer. Finally, we note that the iodine coverage, as determined from x-ray fluorescence, is constant throughout the experiment (bottom panel Figure 2). This last observation is consistent with previous UHV and electrochemical studies by Hubbard and co-workers.[21]

XSW experiments were carried out at the same potentials as before and under conditions of Bragg diffraction and specular reflection. This allows for a determination of the distribution of interfacial species on two different length scales. The results of these measurements are consistent with having a deposited layer of copper on the platinum surface and, in the case of the no-rinsing experiments, an additional amount of copper is present in a region proximal to the electrode surface. These results are fully consistent with those derived from the previously mentioned isotherms.

B. Reflectivity measurements

Reflectivity measurements were carried out to characterize important structural features of the substrate. From a reflectivity measurement one can determine the thickness of the thin solution layer trapped between the LSM and the polypropylene film encapsulating the electrochemical cell, and the LSM's interfacial and surface roughness. Figure 3 shows the angular dependence of the measured absolute Bragg reflectivity for a platinum/carbon LSM under a solution layer 0.98 μm thick. From fits to the Bragg reflectivity measurements we determined the interfacial roughness to be 6.8±0.5Å. Assuming this roughness value for the surface, produced a good fit to the specular reflectivity data as well. We can compare this reflectivity determined surface roughness to that expected for a surface with a random distribution of monatomic steps. In this case we assume a Gaussian distribution whose half-width, σ, is representative of the rms surface roughness in atomic units for this model surface. If we take this value and

multiply it by the closest packing distance for platinum (2.26 Å), in order to place the probability function $\rho(z)$ on an ångstrom scale, we obtain a value of 6.28 Å, which is in excellent agreement with the value of 6.8±0.5Å found by fitting the specular reflection profile. This correlation indicates that a randomly monatomic stepped surface is a reasonable model for the surface of the Pt/C LSM. This result is also consistent with the voltammetric results previously mentioned.

C. XSW measurements:

We now turn to an analysis of the standing wave fluorescence data corresponding to the rinsing experiments discussed above. Specifically, we measured the standing wave profiles for both specular reflection and Bragg diffraction after deposition at potentials of +0.25, +0.20, +0.15 and +0.10 V and rinsing the electrode with clean supporting electrolyte (no copper present in solution) while maintaining potential control over the system at all times. The background subtracted Cu K_α XSW fluorescence yield was extracted from each fluorescence spectrum (in energy dispersed form) by fitting to a Gaussian on a quadratic background. These data were then χ^2 fitted to the theoretical yields. The free parameters in these fits were: the distribution's peak position with respect to the substrate's surface, the distribution's FWHM, and a normalizing constant directly proportional to the distribution's area. In addition, XSW data from the specular and Bragg reflection regions were fitted simultaneously. The best theoretical fits are shown as solid lines on Figure 4 for applied potentials of +0.10 and +0.20 V.

In specular reflection XSW, the first antinode reaches the surface at the critical angle. At the LSM's critical angle the standing wave period D_C is about 100 Å. Keeping the above discussion in mind, we note that in all cases studied, the Cu fluorescence yield peaks at the critical angle of the LSM. This means that a narrow distribution of copper exists at the LSM surface for all of the potentials investigated. However, the period of the standing wave in this regime is large and limits the resolution to which we can determine the distribution's position and width.

To improve the resolution we can make use of the XSW measurements in the Bragg regime, where the periodicity of the standing wave is essentially equivalent to the LSM's d-spacing. Referring to the insets of Figure 4, we observe rather different XSW profiles as a function of applied potential. The expected yield for a random distribution is proportional to (1+Reflectivity) but in all cases studied, the fluorescence peak amplitude to background ratio is well beyond this random limit, indicating that the copper distribution is fairly narrow on the length scale of the standing wave period which in this case is about 40Å. The changes in the shape of each standing wave profile are representative of changes in the position of this overlayer with potential. Fitting XSW data generated in the specular reflection and the Bragg diffraction regimes simultaneously, allows us to probe the same distribution of species on two rather different length scales and two different z-scale origins, leading to an unambiguous result.

Figure 5 summarizes the standing wave results in terms of the distribution profiles at each potential studied. In the main panel all distribution profiles are normalized to the same peak intensity, while in the inset each distribution is plotted in terms of its relative area. Also shown is the surface density profile of the LSM on a normalized scale as determined from reflectivity data and from which we determined a surface roughness of 6.8Å. Note that the origin of the z scale is defined to be where bulk platinum begins.

An especially revealing way of presenting the data is to plot the center of mass (i.e. the z-position where we reach 50% of the total amount of copper) of each

distribution as a function of surface coverage. This is so because the center of mass is dependent on both the peak position and the FWHM in a given distribution. In order to explain the changes we observe in this parameter we need to consider the surface morphology in terms of the Gaussian model we have chosen to fit the reflectivity data. In this model we consider the fractional concentration of surface sites as a function of position along the z-scale (the Gaussian's area is normalized to one). In addition, we sectioned this concentration profile into bins with a width approximately equal to the closest packing distance for platinum (2.26 Å) in order to introduce a finite size effect. If open surface sites were occupied in a random mode, one would expect a homogeneous copper distribution whose center of mass was always at the same z position, namely the center of the Gaussian representing the surface sites concentration profile (i.e. the position with the largest density of open sites). At the opposite extreme, we have a model in which open surface sites are occupied sequentially with the deepest (closest to z=0 Å) ones first. In this case, the center of mass position would vary with the copper surface coverage. Both of these models are plotted, along with the experimental data in Figure 6 as a function of surface coverage. It is immediately clear that the observed results are in excellent agreement with the model that involves sequential filling of available surface sites with the deepest ones being occupied first. This finding implies that the more favorable surface sites for deposition are the ones closest to the platinum bulk lattice, either because the substrate-deposit interactions are maximized at these sites, or because the interaction with the electric fields present at the interface is greatest at these locations. In addition, deposited copper atoms either diffuse to these positions or the deposition process itself is "catalyzed" by these particular sites.

Furthermore, one needs to consider whether the nature of the deposition process is coverage dependent, since lateral interactions among deposited atoms might become more important as the coverage is increased, and what structural role iodine might play. It is also unclear what structural effect rinsing the electrode surface with pure electrolyte has on the UPD layer. It is likely that some structural rearrangement will be triggered by this rinsing pr[illegible]edure.

2. Cu UPD on Au(100):

As mentioned earlier, these studies were carried out ex-situ so that the electrode was removed from the electrolytic solution during the XSW study.

Prior to any electrochemical studies, a reflectivity profile around the Au(200) reflection was recorded at an incident energy of 10.54KeV resulting in a well defined reflectivity curve [22] (Figure 8) and ascertaining the nearly perfect quality of the gold electrode used in this study. In addition, the width of the reflection curve compared very well with the calculated value.

The electrochemical response of the Au(100) electrode was then obtained in 0.1M H_2SO_4 until the characteristic voltammetric response for a clean and well ordered surface was obtained [18]. Afterwards, the electrode was transferred (with a protective drop of electrolyte) to a copper solution (1mM or 50μM) in 0.1M H_2SO_4 where electrodeposition was carried out. In the first case, deposition was carried out from the 1mM solution of copper and a full monolayer was deposited by holding the potential at +0.10V for 3 min. The electrochemical response for monolayer deposition and stripping was well behaved (Figure 7A). The electrode was removed from solution (under potential control) and rinsed with water. It was then transferred to a special holder and mounted on an Eulerian cradle where XSW experiments were carried out at an incident energy of about 10.54KeV where copper fluorescence could be excited while avoiding any of the L edges of gold. The fluorescence intensity was monitored as function of the angle of incidence around the Au(200) reflection. The fluorescence

yield obtained followed closely the reflectivity profile (1+ Reflectivity), indicative of an incoherent (random) distribution of the electrodeposited copper adlayer.

Subsequently, the experiment was repeated after electrodeposition of a sub-monolayer (ca. 0.40ML) amount of copper from the 1mM copper solution. Contrary to the previous case, a well defined modulation in the fluorescence yield was obtained and from a fit of the measured fluorescence to a theoretical yield function, a coherent position of 0.9 was determined, together with a coherent fraction of about 50%.

Finally, deposition of a copper monolayer was performed from a dilute (50μM) solution of copper. In this case, no discernible deposition peak was observed (as anticipated) whereas the stripping response was extremely sharp (Figure 7B) indicative of a very well defined structure. XSW measurements on this sample again exhibited a very well defined modulation in the x-ray fluorescence intensity. Again, from a fit of the measured fluorescence to a theoretical yield function, a coherent position of 0.89±.02 was determined with a coherent fraction of 0.64±0.06 (Figure 8).

Taking into consideration the radii of gold and copper atoms and the measured coherent position, the copper ad-atoms would appear to be located at four-fold hollow sites on the gold lattice with a Cu-Au distance of 2.73±0.03Å (Figure 9). Models where the copper ad-atoms occupied either a-top or bridge sites (Figure 9) were inconsistent with experimental findings. Although additional measurements will be necessary to unambiguously make this assignment, our results are fully consistent with such an adlayer structure. It should also be mentioned that our findings are at odds with the EXAFS data of Tadjeddine and Tourillon who propose that at monolayer coverage, the copper atoms occupy a-top positions [23].

It is clear that the structure of the copper ad-layer is very strongly dependent on the mode of deposition and this may provide a means of controlling interfacial structure. It will be of great interest to determine if the deposition of bulk amounts of copper under similar conditions gives rise to a coherent deposit and if so, to determine the extent of such coherence. Such studies will be the subject of future experiments.

CONCLUSIONS

We have been able to study in situ, the underpotential deposition of copper on an iodine covered platinum/carbon layered synthetic microstructure, using XSWs generated by specular (total external) reflection and Bragg diffraction. The equilibrium structure of the UPD layer after rinsing of the electrode surface with pure electrolyte is one where the deposited copper density is highest for those surface sites closest to the bulk platinum lattice. In addition, we were able to follow potential dependent changes in the copper surface coverage as determined by independent electrochemical and x-ray measurements. There is excellent agreement between x-ray and electrochemical data for the case of rinsing of the electrode. However, x-ray derived isotherms, in the case of no rinsing reveal the presence of a large excess of electrochemically inactive copper at the solid/solution interface, when compared to the corresponding electrochemically derived isotherms.

In the case of Cu UPD on Au (100) the structure and the coherence of the ad-layer are very strongly dependent on the deposition conditions with a much more ordered and coherent deposit being obtained under slow deposition (from dilute solution) conditions.

ACKNOWLEDGMENTS.

This work was supported by the Army Research Office and the Office of Naval Research and the German Federal Ministry for Science and Technology. D.A. acknowledges a MARC NIH fellowship. J.F.R. acknowledges support by the Ford Foundation. H.D.A. acknowledges support by the J. S. Guggenheim Foundation during a visit to HASYLAB. The authors gratefully acknowledge Dr. W. Uelhoff for

kindly providing the Au(100) single crystal and A. Fattah for assistance in preparation of the crystal. Contributions made by Donna Taylor and Howell Yee are gratefully acknowledged.

REFERENCES

1. a. Kolb, D.M., in H. Gerisher and C. Tobias, eds., Advances in Electrochemistry and Electrochemical Enginneering, Vol. 11, J. Wiley and Sons, New York, 1978.
   b. Adzic, R. Isr. J. Chem. 1979 18, 166.
   c. Adzic, R., in H. Gerisher and C. Tobias, eds., Advances in Electrochemistry and Electrochemical Enginneering, Vol. 13, J. Wiley and Sons, New York, 1985.
   d. Juttner, K.; Lorenz, W.J.; Zeit. Physik. Chemie, 1980, 122, 163.
   e. Lorenz, W.J.; Hermann, H.D.; Wuthrich, N.; Hilbert, F.; J. Electrochem. Soc., 1974, 121, 1167.
   f. Szabo, S.; Int. Tev. Phys. Chem. 1991, 10, 207.
2. a. Schultze, J.W.; Dickertmann, D. Symp. Faraday Soc. 1977, 12, 36.
   b. Salvarezza, R.C.; Vasquez Moll, D.V.; Giordano, M.C.; Arvia, A.J. J. Electroanal. Chem. 1986, 213, 301.
   c. Parajon Costa, B.; Canullo, J; Vasquez Moll, D.V.; Salvarezza, R.C.; Giordano, M.C.; Arvia, A.J. J.Electroanal. Chem. 1988, 244, 261.
3. a. Schultze, J.W.; Dickertmann, D. Surf. Sci. 1976, 54, 489.
   b. Bewick, A.; Thomas, B. J. Electroanal. Chem.1976, 70, 239.
4. a. Hubbard, A.T.; Accts. Chem. Res., 1980, 13, 987.
   b. Yeager, E.B.; J. Electroanal. Chem., 1981, 128, 1600.
   c. Ross, P.N.; Surf. Sci., 1981, 102, 463.
   d. Kolb, D.M.; Zeit. Physik. Chemie N.F., 1987, 154, 179.
   e. Hubbard, A.T.; Chem. Rev., 1988, 88, 633.
   f. Beckmann, H.O.; Gerisher, H.; Kolb, D.M.; Lehnpfuhl, G. Symp. Faraday Soc.1977, 12, 51.
5. a. Magnussen, O.M.; Hotlos, J; Nichols, R.J.; Kold, D.M.; Behm, R.J. Phys Rev Lett. 1990, 64, 2929.
   b. Manne, S.; Hansma, P.K.; Massie, J.; Elings, V.B.; Gewirth, A.A. Science, 1991, 251, 183.
   c. Hachiya, T.; Honbo, H.; Itaya, K.; J. Electroanal. Chem. 1991, 315, 275.
   d. Magnussen, O.M.; Hotlos, J.; Beitel, G.; Kolb, D. M; Behm, R. J.; J. Vac. Sci. Tech. B 9, 1991, 969.
   e. Chen, C-H.; Vesecky, S. M.; Gewirth, A. A.; J. Am. Chem. Soc. 1992, 114, 451.
6. Abruña, H. D. ed. "Electrochemical Interfaces: Modern Techniques for In-Sitiu Interface Characterization" VCH, New York, N.Y. 1991.
7. a. Abruña, H.D.; White, J.H.; Albarelli, M.J.; Bommarito, G.M.; Bedzyk, M.J.; McMillan, M.J. J. Phys. Chem.1988, 92, 7045.
   b. Tourillon, G.; Guay, D.; Tadjeddine, A. J. Electroanal. Chem. 1990, 289, 263.
   c. Tadjeddine, A. J.; Guay, D.; Ladouceur, M.; Tourillon, G. Phys. Rev. Lett. 1991, 66, 2235.
   d. Samant, M. G.; Borges, G. L.; Gordon, J. G.; Melroy, O. R.; Blum, L.; J. Amer. Chem. Soc. 1987, 109, 5970.
8. a. Samant, M.G.; Toney, M.F.; Borges, G.L.; Blum, L.; Melroy, O.R. J. Phys. Chem. 1988, 92, 220.

b. Toney, M.F.; Gordon, J.G.; Samant, M.G.; Borges, G.L.; Wiesler, D.G.; Yee, D.; Sorensen, L.B.; Langmuir, 1991, 7, 796.
9. a. Materlik, G.; Zegenhagen, J.; Uelhoff, W.; Phys. Rev. B, 1985, 32, 5502.
b. Materlik, G.; Schmah, M.; Zegenhagen, J.; Uelhoff, W.; Ber. Bunsenges. Phys. Chem., 1987, 91, 292.
c. Zegenhagen, J.; Materlik, G.; Uelhoff, W.; Jnl. X-Ray Sci. Tech. 1990, 2, 214.
10. Bedzyk, M.J.; Bilderback, D.; White, J.H.; Abruña, H.D.; Bommarito, G.M.; J. Phys. Chem., 1986, 90, 4926.
11. a. Abruña, H. D.; Bommarito, G. M.; Acevedo, D.; Science, 1990, 250, 69.
b. Bommarito, G.M.; White, J.H.; Abruña, H.D.; J. Phys. Chem. 1990, 94, 8280.
12. Bedzyk, M.J.; Bommarito, G.M.; Caffrey, M.; Penner, T.; Science, 1990, 52, 248.
13. a. Batterman, B.W.; Cole, H.; Rev. Mod. Phys., 1964, 36, 681.
b. Batterman, B.W.; Phys. Rev., 1964, 133, A759.
14. Bedzyk, M.J.; Bilderbach, D.H.; Bommarito, G.M.; Caffrey, M.; Schildkraut, J.J.; Science, 1988, 241, 1788.
15. a. P.L. Cowan; J.A. Golovchenko; M.F. Robbins; Phys. Rev. Lett. 1980, 44, 1680.
b. J.A. Golovchenko; J.R. Patel; D.R. Kaplan; P.L. Cowan; M.J. Bedzyk; Phys. Rev. Lett. 1982, 49, 560.
c. Materlik, G.; Zegenhagen, J.; Phys. Lett., 1984, 104A, 47.
16. Underwood, J.H.; Barbee, T.W.; in AIP Conf. Proc., 75, 170, D.T. Atwood, B.L. Henke, eds., AIP, New York, 1981.
17. a. Fehmer, H.; Uelhoff, W.; J. Sci. Instrum. 1969, 2, 767.
b. Fehmer, H.; Uelhoff, W.; J. Sci. Instrum. 1969, 2, 771.
18. Angerstein-Kozlowska, Conway, B. E.; Hamelin, A.; Stoicoviciu, L.; Electrochim. Acta 1986, 31, 1051.
19. Kolb, D. M.; Al Jaaf-Golze, K.; Zei, M. S.; DECHEMA-Monographien Bd. 102 VCH Winheim, 1986.
20. Aberdam, D.; Durand, R.; Faure, R.; El-Omar, F.; Surf. Sci. 1986, 171, 303.
21. a. Stickney, J.L.; Rosasco, S.D.; Song, D.; Soriaga, M.P.; Hubbard, A.T.; Surf. Sci. 1983, 130, 326.
b. Hubbard, A.T.; Stickney, J.L.; Rosasco, S.D.; Soriaga, M.P.; Song, D.; J. Electroanal. Chem. 1983, 150, 165.
c. Stickney, J.L.; Rosasco, S.D.; Hubbard, A.T.; J. Electrochem. Soc. 1984, 131, 260.
22. James, R.W.; The Optical Principles of the Diffraction of X-rays,"Oxbow Press, Woodbridge, Connecticut, 1982.
23. Tourillon, G.; Guay, D.; Tadjeddine, A.; J. Electroanal. Chem. 1990, 289, 263.

Figure Legends:

Figure 1

Cyclic voltammogram at 20mV/s for the UPD of copper on an iodine covered platinum surface of a Pt/C LSM in contact with a 0.1M H_2SO_4 solution solution containing copper at a concentration of 0.1mM.

Figure 2

X-ray and electrochemical derived isotherms plotted on an absolute coverage scale after the two data sets were normalized at one point, +0.1 V after rinsing.
Bottom panel: Normalized iodine fluorescence as a function of applied potential.

Figure 3

Angular dependence of the measured absolute Bragg reflectivity (filled circles) for a Pt/C LSM under a solution layer 9800Å thick, encapsulated by a 6.35mm polypropylene film. The dashed line represents the theoretical prediction for the reflectivity when the interfacial roughness of the substrate is neglected. The dottted line represents a calculation attempting to fit the experimental data by increasing the solution layer thickness, while continuing to neglect the interfacial roughness. The solid line represents the best fit to the data when including interfacial roughness.

Figure 4

The XSW fluorescence profiles for both the specular reflectivity and Bragg diffraction regimes for +0.10V and +0.20V after rinsing the electrode surface with clean electrolyte. A magnified view of the Bragg data is show in the insets. Also shown at the bottom, is the complete reflectivity profile. Fits of the data were performed over the entire angular range simultaneously, and are plotted as solid lines.

Figure 5

Copper concentration profiles (after rinsing) vs. distance z normal to the LSM's surface, derived from the analysis of the standing wave data. In the main panel all distributions are normalized so that the peak concentration is one. The inset shows the same concentration profiles in terms of their relative areas.

Figure 6

Variation of the center of mass in the copper ad-layer as a function of surface coverage. Curve A represents the expected variation in the center of mass for a model in which filling of the surface sites is random, whereas B represents the variation expected for a model where the surface sites are filled sequentially starting with the deepest ones (closest to z=0 Å) first. Points are experimental data.

Figure 7

A. Cyclic voltammogram at 20 mV/s for a Au(100) electrode in contact with a 0.1M H_2SO_4 solution containing copper at a concentration of 1mM.
B. Cyclic voltammogram at 20 mV/s for a Au(100) electrode in contact with a 0.1M H_2SO_4 solution containing copper at a concentration of 50μM after holding the potential at +0.10V for 3 minutes.

Figure 8

XSW measurement of copper electrodeposited on a Au(100) electrode from a 0.1MH_2SO_4 solution containing 50μM copper sulfate. Shown are the reflectivity (o) and the Cu K_α fluorescence (•) along with fitted theoretical lines.

Figure 9
Pictorial depiction of the structure of electrodeposited copper on a Au(100) surface comparing the copper ad-atoms occupying either bridge or four-fold hollow sites.

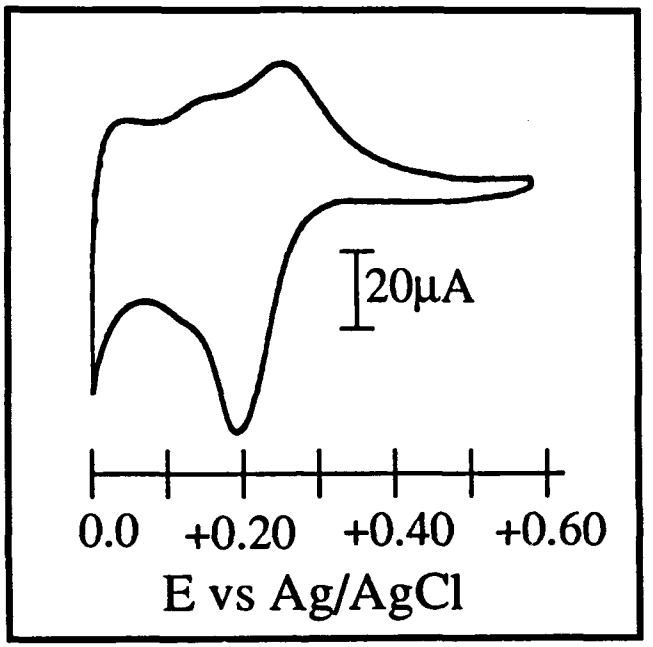

Figure 1

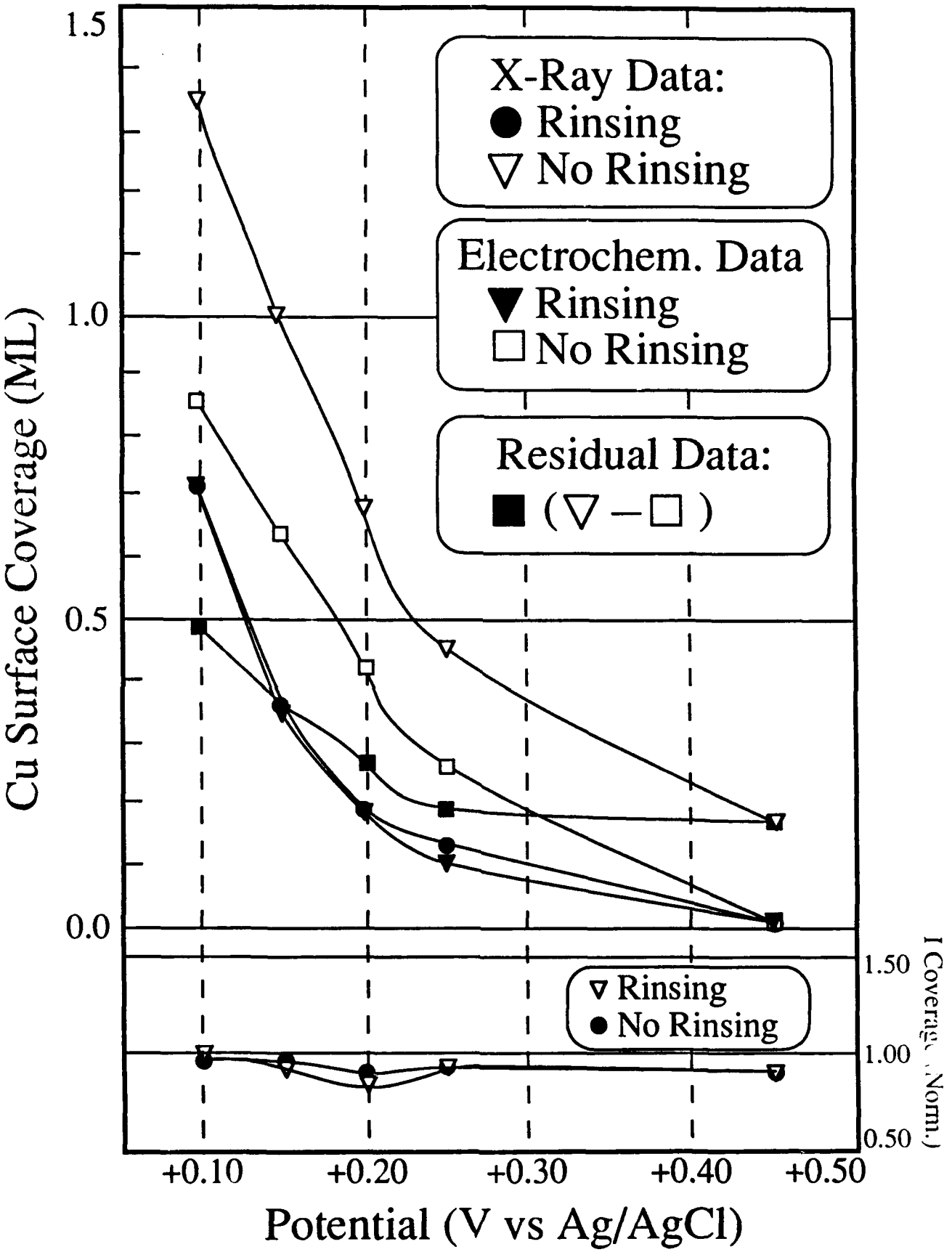
X-Ray Data:
● Rinsing
▽ No Rinsing
Electrochem. Data
▼ Rinsing
□ No Rinsing
Residual Data:
■ (▽ − □)
▽ Rinsing
● No Rinsing
Cu Surface Coverage (ML)
1.5
1.0
0.5
0.0
1.50
1.00
0.50
+0.10
+0.20
+0.30
+0.40
+0.50
Potential (V vs Ag/AgCl)

Figure 2

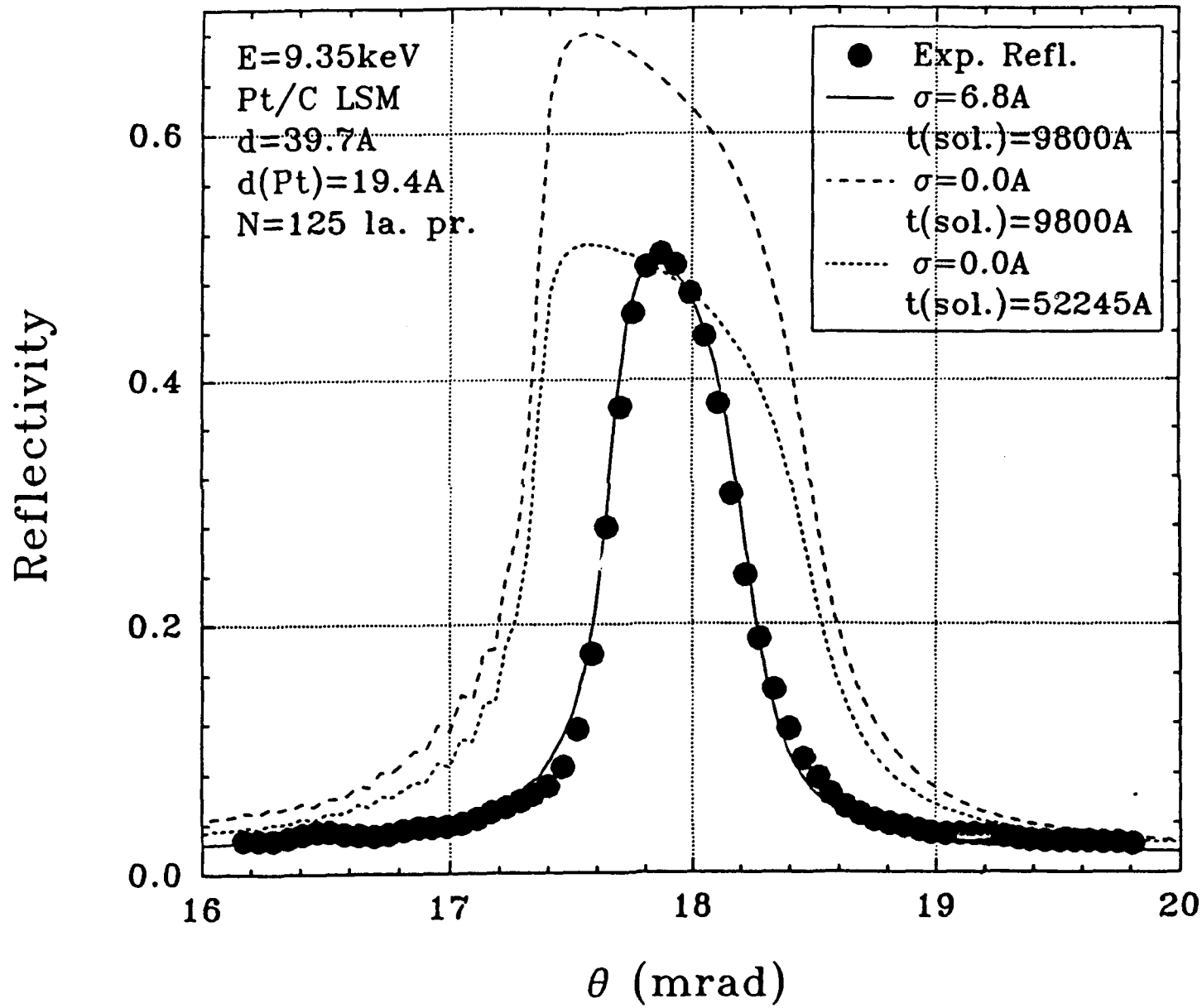
E=9.35keV
Pt/C LSM
d=39.7A
d(Pt)=19.4A
N=125 la. pr.
Exp. Refl.
σ=6.8A
t(sol.)=9800A
σ=0.0A
t(sol.)=9800A
σ=0.0A
t(sol.)=52245A
Reflectivity
0.0
0.2
0.4
0.6
16
17
18
19
20
θ (mrad)

Figure 3

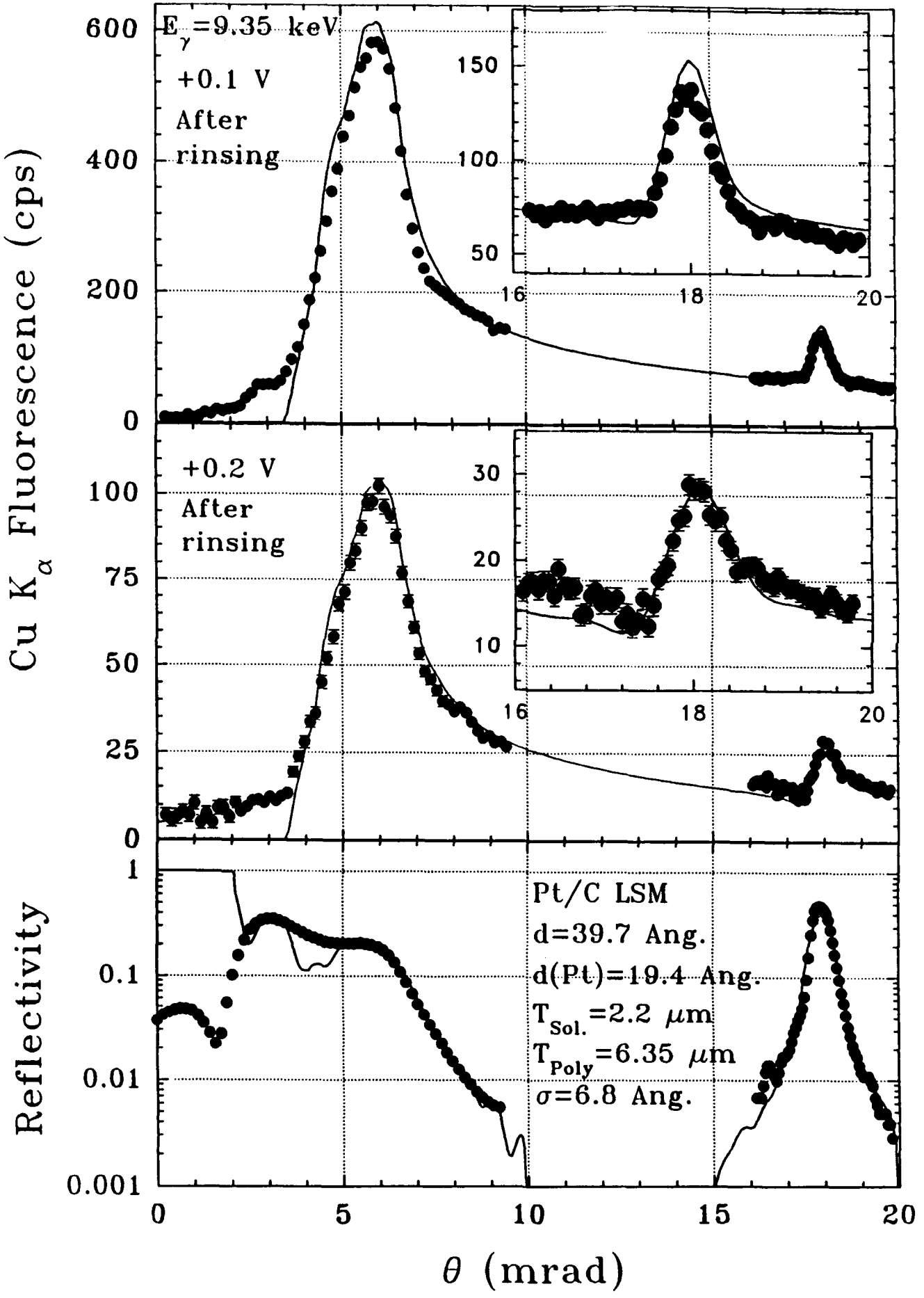
E$_\gamma$=9.35 keV
+0.1 V
After
rinsing
+0.2 V
After
rinsing
Cu K$_\alpha$ Fluorescence (cps)
Reflectivity
Pt/C LSM
d=39.7 Ang.
d(Pt)=19.4 Ang.
T$_{Sol.}$=2.2 μm
T$_{Poly}$=6.35 μm
σ=6.8 Ang.
θ (mrad)

Figure 4

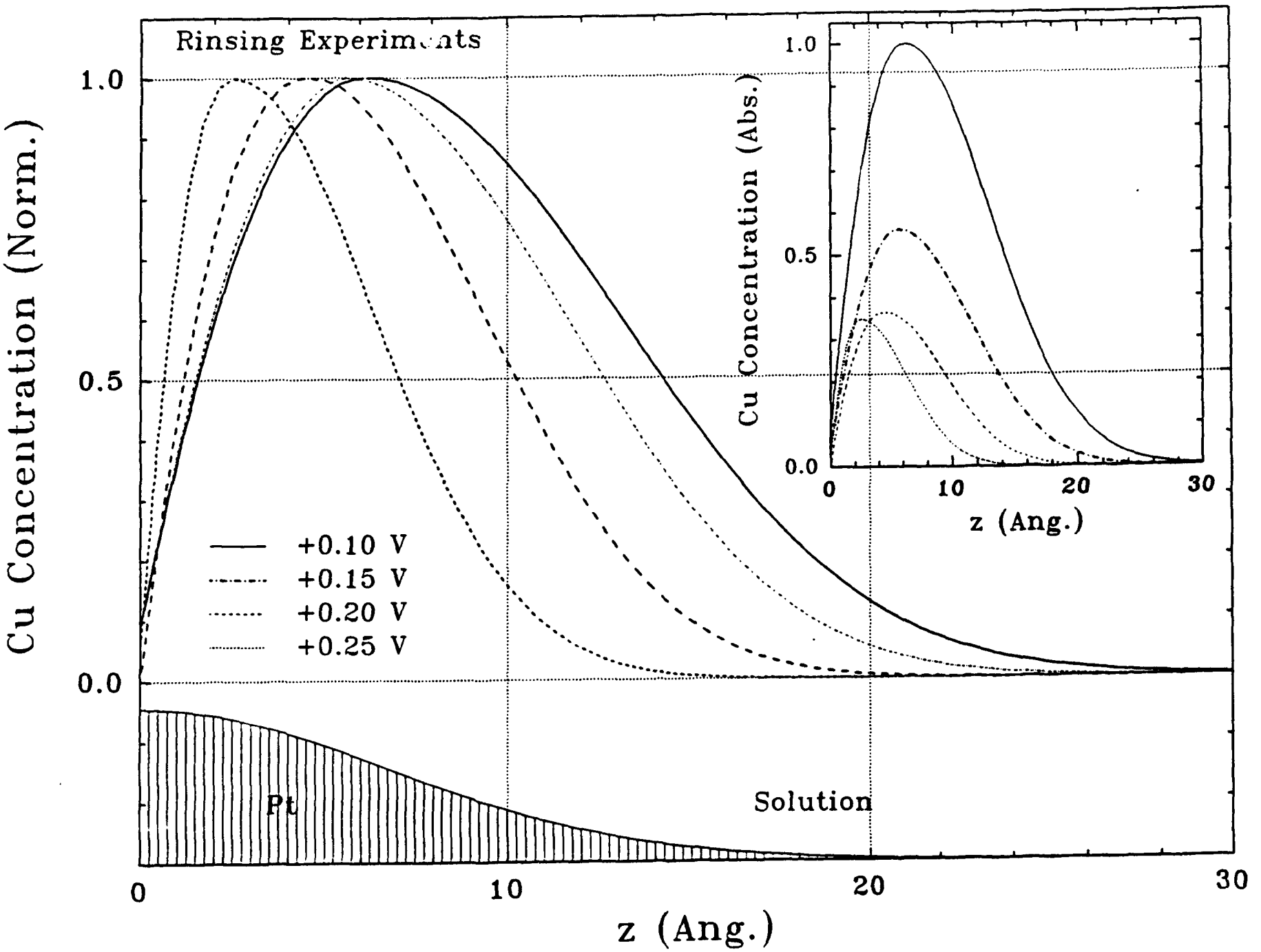
Rinsing Experiments
Cu Concentration (Norm.)
1.0
0.5
0.0
+0.10 V
+0.15 V
+0.20 V
+0.25 V
Pt
Solution
0
10
20
30
z (Ang.)
Cu Concentration (Abs.)
1.0
0.5
0.0
0
10
20
30
z (Ang.)

Figure 5

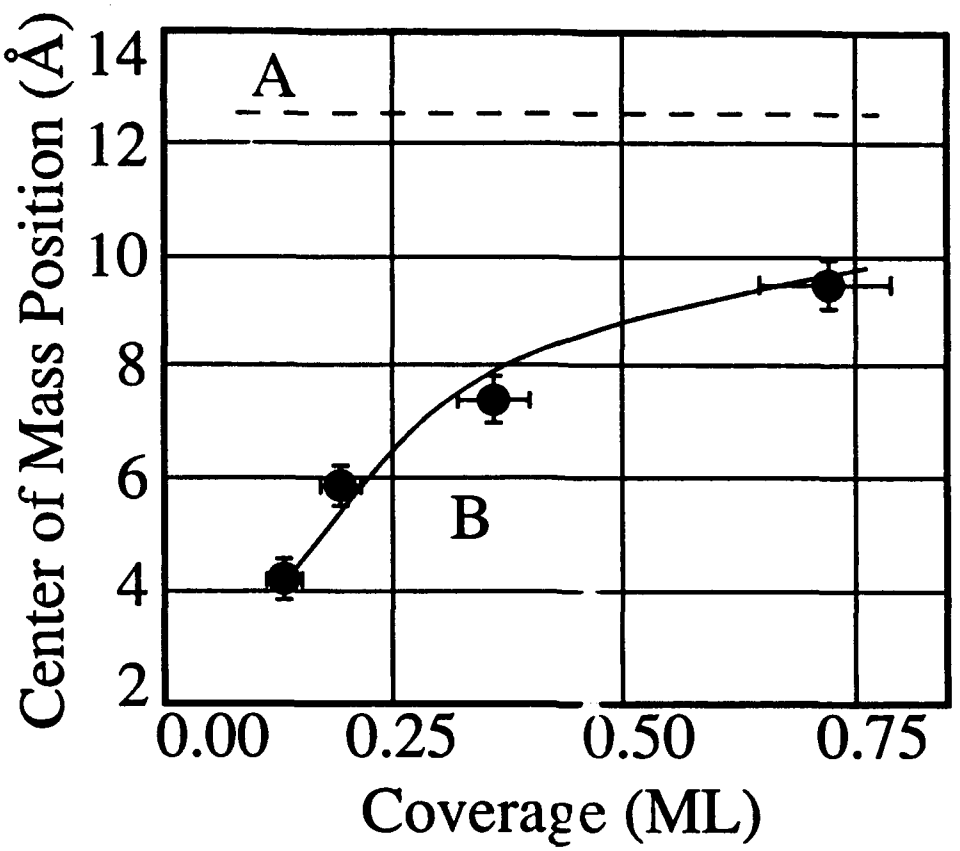
Center of Mass Position (Å)
14
12
10
8
6
4
2
A
B
0.00
0.25
0.50
0.75
Coverage (ML)

Figure 6

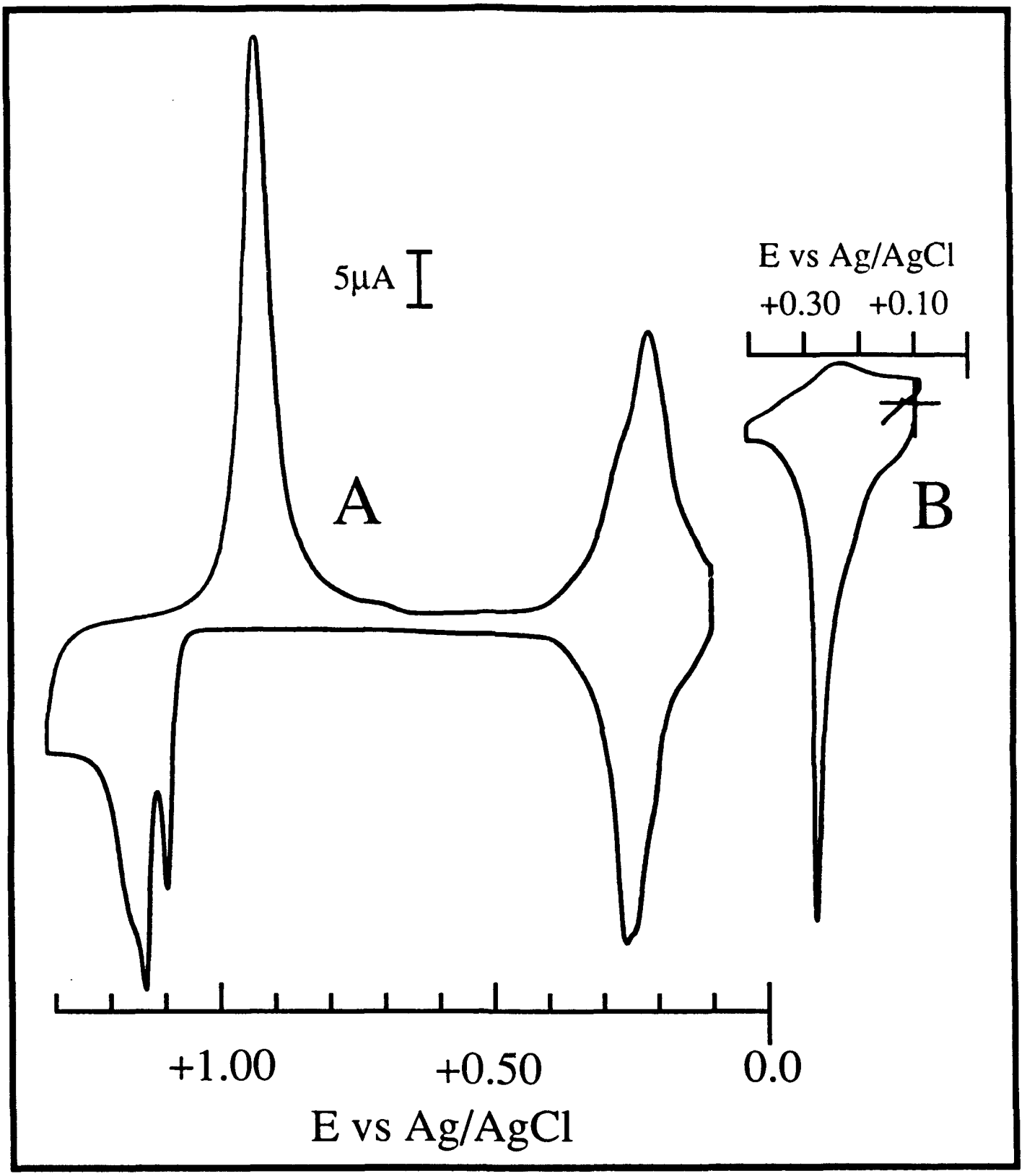

Figure 7

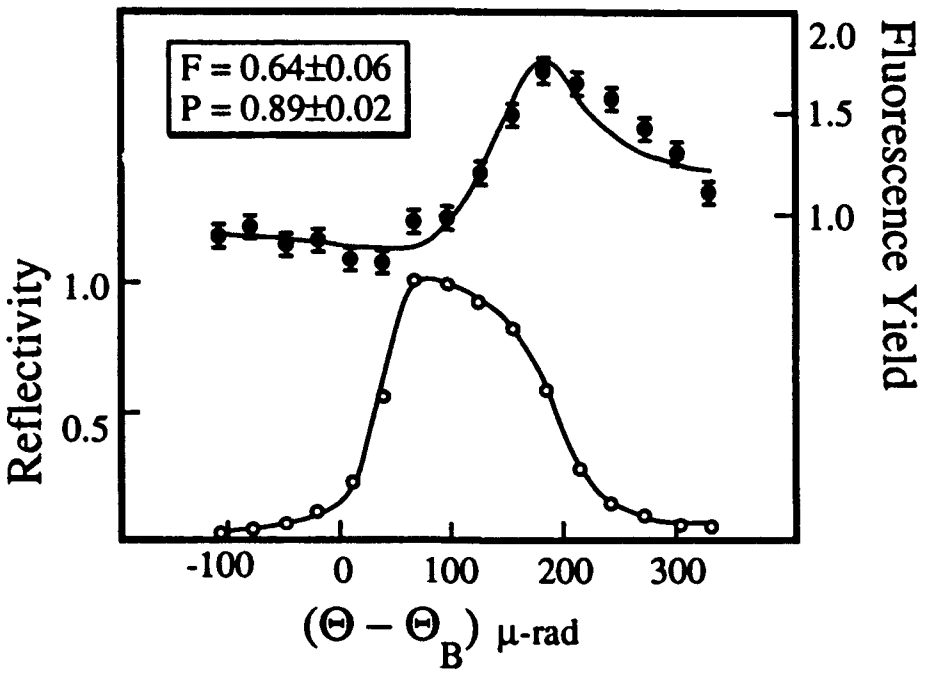
F = 0.64±0.06
P = 0.89±0.02
Reflectivity
1.0
0.5
2.0
1.5
1.0
Fluorescence Yield
-100
0
100
200
300
(Θ − Θ_B) μ-rad

Figure 8

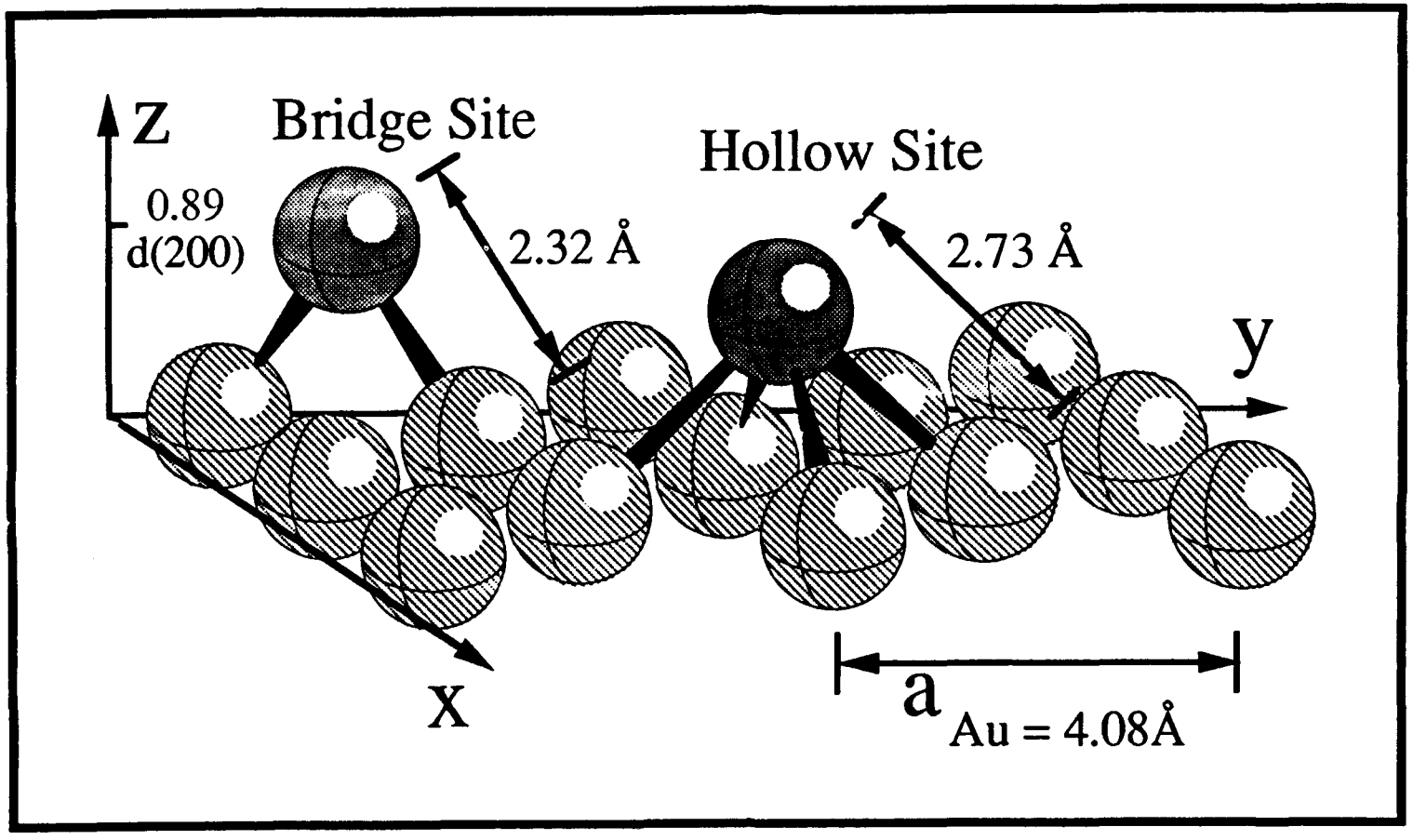

Figure 9